Physics of the Solid State, 2022, Vol. 64, No. 11

05,11,04

Features of structure distortion at a phase transition in diluted $YBaCo_{4-y}Zn_yO_{7+x}$ ($y = 0, 0.3$) cobaltites

© Z.A. Kazei[1], V.V. Snegirev[1], M.S. Stolyarenko[1], K.I. Kamilov[1,2], L.N. Khanov[2]

[1] Moscow State University,
Moscow, Russia
[2] Amirkhanov Institute of Physics, Dagestan Federal Research Center, Russian Academy of Sciences,
Makhachkala, Russia

E-mail: kazei@plms.phys.msu.ru

Received July 4, 2022
Revised July 4, 2022
Accepted July 6, 2022

Experimental studies of the lattice parameters, thermal expansion, and elastic characteristics in the range of the structural phase transition in the $YBaCo_{4-y}Zn_yO_{7+x}$ series of cobaltites with diamagnetic dilution of the cobalt subsystem have been carried out. It has been found that for stoichiometric samples annealed in vacuum, the parameter $\Delta a/a$ shows no features during the structural transition, while the parameters $\Delta b/b$ and $\Delta c/c$ experience similar jumps of different signs. This leads to a jump in anisotropic (rhombic) $\varepsilon_o \approx -4 \cdot 10^{-3}$ and isotropic (volume change) $\Delta V/V \approx -1 \cdot 10^{-3}$ deformations. Upon substitution with Zn ions, the orthorhombic distortion of the structure changes slightly, and the jump in the volume anomaly (linear thermal expansion) changes sign. Structure distortion in stoichiometric samples is accompanied by characteristic anomalies in the Young's modulus $\Delta E(T)/E_0$ and internal friction in the T_S range, while for nonstoichiometric quenched samples, the anomalies completely disappear. The diamagnetic substitution with Zn ions leads to a sharp decrease and then complete disappearance of the jump in the curve $\Delta E(T)/E_0$. This may be due to a change in the ratio of isotropic and anisotropic deformation during the structural transition upon a small substitution in the cobalt subsystem.

Keywords: frustrated systems, cobaltites, structural phase transitions, lattice parameters, isotropic deformation, anisotropic deformation, thermal expansion, Young's modulus, internal friction.

DOI: 10.21883/PSS.2022.11.54198.420

1. Introduction

Geometrically frustrated systems are still a target of many experimental and theoretical research activities in recent years [1,2]. The most studied systems are antiferromagnetics with the Kagome lattice and pyrochlore structure that have disordered ground states [3,4]. It was shown that various weak disturbances in these systems, such as minor distortions of structure, interactions with secondary neighbors, local anisotropy, etc., may have a pronounce effect on the degeneration of the ground state and result in a state with a long-range magnetic order.

Rare earth (RE, R) cobaltites, that simultaneously have in their structure alternating triangular levels and Kagome layers, demonstrate unusual magnetic behavior due to the frustration of exchange interactions and variable valence in the cobalt subsystem [5–10]. The compounds like these make it possible to study fundamental problems of solid state physics and magnetism, such as nontrivial ground states, effects of short-range order, as well as complex magnetic structures, spontaneous and induced phase transitions of different nature.

$RBaCo_4O_{7+x}$ layered cobaltites are formed by Y, Ca ions and heavy RE-ions starting with Tb. Stoichiometric compounds with the R^{3+} trivalent ion contain mixed valence cobalt ions, Co^{2+} and Co^{3+}, in a proportion of $3:1$, which are distributed in the structure in a disordered manner over two types of tetrahedral sites. The aliovalent ions ratio of Co^{2+}/Co^{3+} in a cobalt subsystem can be varied using non-isovalent substitution of $R^{3+} \to Ca^{2+}$ or $Co^{2+}/Co^{3+} \to Zn^{2+}/Al^{3+}$, as well as a change in oxygen content $(7 + x)$.

Crystalline structure of RE-cobaltites at high temperatures is described by a hexagonal $P6_3mc$ (or trigonal $P31c$) space group [11–15]. In the crystalline framework the CoO_4 tetrahedra united by common corners form triangular layers and the Kagome layers alternatively packed along the c axis. Larger octahedral and cuboctahedral sites in a three-dimensional tetrahedral lattice are occupied by R^{3+} and Ba^{2+} cations, respectively. In an infinite flat lattice of bound triangles frustration in the magnetic system results in a degenerated ground state and absence of a long-range magnetic order even at considerable constants of exchange interaction [16]. A minor distortion of structure in stoichiometric RE-cobaltites removes the frustration of exchange interactions, that promotes the development of a long-range magnetic order in the Co-subsystem below the temperature T_S of structural transition [17,18].

Y-cobaltite containing one type of magnetic ions undergoes structural transition at $T_S = 313\,K$, making the symmetry lowered from hexagonal to orthorhombic (space group $Pbn2_1$; $a_o \approx a_h$, $b_o \approx \sqrt{3}a_h$) and accompanied by anomalies of elastic, magnetic and transport properties. Critical temperature of structural transition T_S of cobaltites with magnetic RE-ions decreases in a monotone manner with a decrease in RE-ion radius [19–23]. Below the structural transition in $YBaCo_4O_7$ an emergence of three-dimensional antiferromagnetic ordering is observed in the Co-subsystem at the Neel point of $T_N \approx 110\,K$ with symmetry lowering down to monoclinic $P112_1$ [5,16,24]. With further temperature decrease one more magnetic phase transition is observed at $T_{N2} \approx 70\,K$ [25], which is attributable to the spin flip in the Co-subsystem [16]. Due to the frustration of exchange interaction, the long-range magnetic order is established at a temperature that is considerably lower than the Curie−Weiss paramagnetic temperature $\theta_{CW} = -508\,K$ and is characterized by a complex noncollinear magnetic structure [5,16].

The crystalline structure of layered cobaltite is studied in reasonable detail in the hexagonal phase and considerably less studied in the distorted orthorhombic phase. Currently the issue of nature and mechanism of the structural transition still remains open. Different models are discussed, such as charge ordering in the Co-subsystem [19], optimization of saturated bonds of Ba-coordination polyhedron [14], spin-lattice instability and even the emergence of short-range antiferromagnetic order/correlations in the Co-subsystem [21].

Refinement of structural parameters has revealed a large size of the Co1 site as compared with Co2, $\langle d \rangle_{Co1-O} > \langle d \rangle_{Co2-O}$, within two assumed models of distorted phase $Pbn2_1$ and $Cmc2_1$. This is an argument against the Co1 valence greater than that of Co2 and does not confirm the ideas of charge ordering at phase transition [26]. The authors of [14] have made an assumption that the transition in $YbBaCo_4O_7$ cobaltite is a consequence of unsaturated bonds of Ba^{2+} ions in the high-temperature phase. In [26] the transition at T_S is classified as a transition of displacement type in the tetrahedral lattice and attributed to the condensation of librational phonon phase connected with the rotation of tetrahedra as complete items inside starlike tetrahedral units that are building blocks of the Kagome lattice. Phase transitions in tetrahedral lattices occurring as displacements [27] are often caused by soft optical phonons. These modes can propagate without the distortion of tetrahedra [28] (rigid-unit modes or RUM) [29] and are the most typical for systems that contain chains of tetrahedra.

The character of the change in lattice parameters (lattice metric) at the structural transition, as well as the change in transition temperature and magnitude of distortion at different substitutions in Co- and RE- sublattice or deviation from stoichiometry are not sufficiently studied. The effect of structure distortion on the behavior of the frustrated Co subsystem was studied for a series of Y-cobaltites with minor deviation from stoichiometry [30]. In this work we study the effect of diamagnetic dilution in a frustrated cobalt subsystem on structural phase transitions, as well as structural and elastic characteristics in a series of layered cobaltites, $YBaCo_{4-y}Zn_yO_{7+x}$, close to stoichiometric ones.

2. Samples and experiment technique

Structural and elastic properties were studied on polycrystalline samples of $YBaCo_{4-y}Zn_yO_{7+x}$ $(y = 0.1,\ 0.2.\ 0.3)$ synthesized by ceramic technology. The synthesis was conducted in three stages at temperatures of 900, 1000, and 1100°C with quenching at the end of annealing and in intermediate rubbing through (see [31] for details).

After the synthesis and quenching from 900−950°C the $RBaCo_4O_{7+x}$ ceramics as a rule have an excess of oxygen. In case of $YBaCo_{4-y}Zn_yO_{7+x}$ system the quenched Q samples had a slight excess of oxygen $x \leq 0.07$, and to obtain stoichiometric homogeneous A samples with $x \approx 0$, they were annealed in vacuum at 500°C [31,32]. After annealing, the deviation from stoichiometry by oxygen became negative (deficiency) and noticeably reduced by absolute value for all samples under study. Thus, despite the samples after vacuum annealing were slightly non-stoichiometric, the deviation x was noticeably lower. The substitution of Co^{2+} atoms with Zn^{2+} atoms in tetrahedra (ion radii equal to 0.74 and 0.72 Å, respectively) results in a systematic increase in parameters of the crystalline lattice of the annealed samples. The annealed samples, to our opinion, are close to equilibrium in terms of distribution of Zn^{2+} ions and non-stoichiometric oxygen. The studies show that structural and magnetic transitions in these samples are more sharp.

The oxygen content in the samples was determined by iodimetric titration [33] in a software-controlled original automated setup (see [22] for detailed description). Two-three successive experiments were carried out for each sample, where $\sim 30\,mg$ of the sample under study were solved in 1.5-M solution of HCl containing an excess of KI. Reduction of Co^{3+} high-valent ions of the sample to Co^{2+} ions resulted in the formation of a stoichiometric quantity of iodine in the solution, which was titrated by 0.02-M solution of $Na_2S_2O_3$ dosed by an electronic piston burette. The final point of titration (the equivalent point) was determined by a step in a potential in the process of chemical reaction when measuring e.m.f. of the reversible cell. Relative error of oxygen deviation x from the stoichiometry is $\sim 1.5\%$.

X-ray studies at a room temperature were carried out using the Stoe Stadi P diffractometer with a monochromator on the primary beam ($CoK_{\alpha 1}$ radiation). Temperature X-ray measurements were carried out using the Rigaku Geigerflex diffractometer on $CoK_{\alpha 1,\alpha 2}$ or $FeK_{\alpha 1,\alpha 2}$ radiation without a monochromator with a low-temperature chamber of Oxford_Instruments (England), in a range of 77−350 K. The X-ray pattern was analyzed in an angular range of 18−120° at temperatures of 300 and 80 K by the Rietveld method using Full_Prof software. This made it possible to determine values of a, b, and c parameters in a hexagonal or slightly distorted hexagonal (orthorhombic) lattice cell (hereinafter a, b, c notations are used for parameters of the orthorhombic cell). The quality of X-ray pattern description was defined by the magnitude of integral difference function χ^2. Temperature measurements of three lattice parameters of the rhombic structure were carried out using two closely located (split) reflections $(260)+(400)$ and reflection (004) with angles of $2\theta_{1,2} \approx 69^\circ$ and $2\theta_3 \approx 41^\circ$, respectively.

Heat expansion was measured by the strain-gauge method in a temperature range of $77-320$ K in heating and cooling modes. For the measurements one pressure-sensitive resistor was glued on a face of the sample under study, while another, compensating, pressure-sensitive resistor was glued on a quartz plate. Both pressure-sensitive resistors were connected into the Wheatstone bridge legs. Resistances of working and compensating pressure-sensitive resistors were different by not more than $0.1\,\Omega$. The change in sample length due to heat expansion results in a change of resistance of the working pressure-sensitive resistor and disturbance of the bridge equilibrium. The emerging voltage difference in the bridge diagonal was measured by a multimeter.

The Young modulus E and internal friction coefficient q^{-1} were measured by the composite resonator method at a frequency of ~ 100 kHz in a steady-state mode (accuracy of temperature measurement was ± 0.03 K) in a temperature range of $80-300$ K in an original automated setup (see [22] for more detailed description). Temperature dependencies of amplitudes and antiresonance frequencies on a smoothed experimental amplitude frequency response function $A_{\mathrm{sm}}(f)$ made it possible to determine the change in the Young modulus $E(T)$ and absorption (internal friction coefficient) $q^{-1}(T)$ in a wide range of temperatures.

3. Experimental results and discussion

3.1. X-ray diffraction analysis and heat expansion

Studies of the structure allow identifying the features of phase transition in the $\mathrm{YBaCo}_{4-y}\mathrm{Zn}_y\mathrm{O}_{7+x}$ system, i.e., the dependencies of temperature, character, and magnitude of distortion on substitution y. For the $\mathrm{YBaCo}_{4-Y}\mathrm{Zn}_y\mathrm{O}_{7+x}$ sample with $y = 0.3$ all lines on the X-ray pattern at a room temperature are indicated within the hexagonal structure. In X-ray patterns of this sample at $T = 80$ K and unsubstituted $\mathrm{YBaCo}_{4-Y}\mathrm{O}_{7+x}$ at $T = 300$ K a significant difference is observed for a number of reflections (the highest difference is observed for reflections with angles of $2\theta \approx 63$ and 69°) sensitive to rhombic distortion). At the same time their structure is described taking into account minor rhombic distortion.

Measurement of the full X-ray pattern with good statistics at different temperatures requires significant time. If the character of the structure distortion is determined and remains unchanged with temperature increase, then it is sufficient to measure temperature positions of three peaks to study parameters of the distorted rhombic lattice. A strong peak sensitive to rhombic distortion $(400)+(260)$ with a Bragg angle of $2\theta = 69^\circ$ gives information about the presence of distortions in the sample. To study minor rhombic distortion of the structure, this peak was measured in an interval of $80-305$ K. The peak was processed using one of the utilities of Stoe_WinXPow_Profile_Fitting software. Experimental peaks were approximated by the pseudo-Voigt function, and optimum description of split peak profile was determined by the minimum value of the difference function χ^2.

Let us consider in more detail the distortion of structure for the sample of Y-cobaltite with a dilution of $y = 0.3$. The split of reflection $(400)+(260)$ sensitive to rhombic distortion directly gives the following distortion

$$\varepsilon_o = (a - b/\sqrt{3})/a = 2(d_1^2 - d_2^2)/(4d_1^2 - d_2^2),$$

where $d_{1,2}^{-1} = 2\sin(\theta_{1,2})/\lambda$, a $\theta_1 = \theta_{400}$, $\theta_2 = \theta_{260}$ — Bragg angles of corresponding reflections. At $T = 300$ K on the $\mathrm{CoK}_{\alpha1,\alpha2}$ radiation an unsplit doublet reflection is observed for $d_1 = d_2$ at $b = a\sqrt{3}$, while below 260 K this reflection demonstrates splitting into two lines. At the same time the high-angle component of the split reflection with $2\theta_2$ remains in place and an additional line arises shifted by $\Delta(2\theta_1) \approx 0.25^\circ$. The split of reflection with an angle of $2\theta_{1,2} \approx 69^\circ$ arises in a stepwise manner at a temperature of phase transition $T_{\mathrm{S}} \approx 260$ K and slightly decreases at temperature lowering down to 80 K. The complex profile of the split line is described by two doublets with the split components intensity ratio of $2:1$, that corresponds to the statistic value for this type of distortion.

Reflection (004) allows determining the change of the parameter c depending on temperature. The Bragg angle $2\theta_3 \approx 41^\circ$ increases in a stepwise manner by $\Delta(2\theta_3) \approx 0.2^\circ$ at T_{S} and continues to increase at temperature lowering down to 80 K. This reflection remains unsplit at the rhombic distortion of the lattice and its double structure in the region of T_{S} reflects the two-phase state of the sample, when two phases exist in a range of ~ 10 K. The presence of a two-phase state near T_{S} on the reflection with an angle of $2\theta_{1,2} \approx 69^\circ$ is manifested as an increase in intensity I_2 of the high-angle component, on which a reflection of hexagonal phase is superimposed with the same Bragg angle (see inset in Fig. 1). In the region of two-phase state relative intensity $I_1/(I_1 + I_2)$ of the low-angle component decreases, while intensity $I_2/(I_1 + I_2)$ of the high-angle component increases, so the ratio of intensities does not correspond to the statistic ratio of $2:1$.

Dependencies of cell parameters for the sample with $y = 0.3$, obtained by processing of peaks at different temperatures in a range of $80-305$ K are shown in Fig. 1. For the ease of comparison of all lattice parameters $\Delta a/a$, $\Delta b/b$, $\Delta c/c$, volume $\Delta V/V$ and magnitudes of rhombic distortion $(\varepsilon_o = \Delta a/a - \Delta b/b)$ the following figures illustrate their relative changes normalized to the values of the corresponding parameter at T above T_{S}, for example, $\Delta a/a = \Delta a(T)/a_0$ $(\Delta a(T) = a(T) - a_0;$ $a_0 = a(T = 300\,\mathrm{K}))$.

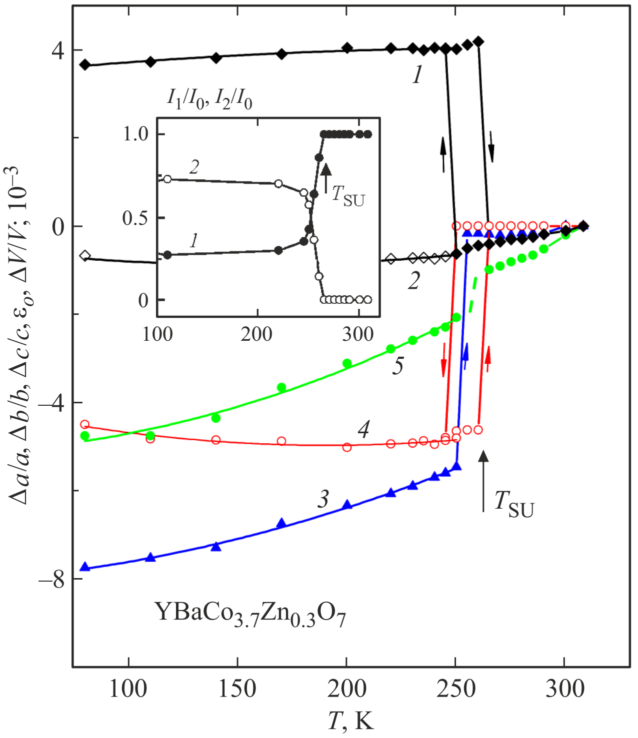

Figure 1. Relative changes of lattice parameters and symmetrical strains (curve *1* — $\Delta a/a$, *2* — $\Delta b/b$, *3* — $\Delta c/c$, *4* — ε_o, *5* — $\Delta V/V$) with the temperature of stoichiometric substituted sample $YBaCo_{4-y}Zn_yO_{7+x}$ at a dilution of $y = 0.3$. All dependencies are normalized to parameter values at $T = 300\,K$: $\Delta a_i/a_i = (a_i(T) - a_{i0})/a_{i0}$, $a_{i0} = a_i(T = 300\,K)$; $a_i = a, b, c, \varepsilon_o, V$. The inset shows dependencies of relative intensity of components (400) (I_1/I_0, curve *1*) and (260) (I_2/I_0, curve *2*) of the split peak at phase transition.

Let us consider the character of change of the lattice metric at phase transition for the sample with $y = 0.3$ (Fig. 1). It is interesting to note, that at phase transition the parameter a does not undergo any stepwise changes and changes a little in magnitude. While heating, the parameters b and c demonstrate stepwise changes with different signs and comparable magnitudes $\Delta b/b \approx -4 \cdot 10^{-3}$ and $\Delta c/c \approx 5 \cdot 10^{-3}$, that results in a small step in volume $\Delta V/V \approx 1 \cdot 10^{-3}$. Below the transition temperature the parameters b and a change poorly, parameter c decreases with the decrease in temperature. The range of the two-phase state determined by the parameter c is $\sim 265{-}270\,K$. Above T_S (in the hexagonal phase) the parameters a and $b' = b/\sqrt{3}$ coincide with each other. For the unsubstituted sample with $y = 0$ the temperature T_S is above the room temperature, while maximum distortion ε_o and parameter change $\Delta c/c$ in a range of $80 - T_S\,K$ and their steps at T_S are slightly decreased (see further).

In case of substitution the character of splitting and reflection changes at structural transition generally remains the same, changing are only the magnitudes of lattice distortions and parameter steps. It is worth noting, that for the substituted sample, as well as for unsubstituted sample, the ratio of component intensities of the split reflection with $2\theta_{1,2} \approx 69^\circ$ at a rhombic distortion of the structure corresponds to the statistic ratio of $2:1$. This is indicative of keeping the sign of rhombic distortion unchanged. The lattice cell is expanded along one of 2-nd order axes normal to the hexagonal axis, while the size of the cell along other two equivalent axes remains unchanged.

It is common to describe the highest lattice strain at a structural transition in terms of anisotropic (change in degree of rhombic distortion) $\varepsilon_o = (\Delta a/a - \Delta b/b)$ and isotropic (change in volume) $\Delta V/V = (\Delta a/a + \Delta b/b + \Delta c/c)$ strains. The anisotropic strain, as it was already said before, is unambiguously defined by splitting of reflection $(400) + (260)$ and can be measured with a sufficient precision, because the systematic error connected with sample misadjustment does not affect the precision of measurements. The change in volume at a condition of $\Delta a/a \approx 0$ is defined, as can be seen from the formula, by parameter steps $\Delta b/b$ and $\Delta c/c$, which have their magnitudes close to each other, but with different signs. Therefore the volume step $\Delta V/V$ at phase transition is small, and its error is significant. So, to analyze the change in the lattice strain at phase transition depending on y substitution by ions of Zn, in the following we use values of ε_o and $\Delta c/c$.

In case of pure unsubstituted sample with $y = 0$, phase transition is accompanied by stepwise changes in the degree of rhombic distortion $\varepsilon_o \approx -4 \cdot 10^{-3}$ and parameter $\Delta c/c \approx -4 \cdot 10^{-3}$ (Fig. 2), as well as volume $\Delta V/V \approx 10^{-3}$. With the decrease in temperature from $T \leq T_S$ the parameter c decreases, parameter b remains almost unchanged, and parameter a, in contrast, has a little increase (negative heat expansion), that results in the decrease in the degree of rhombic distortion $\varepsilon_o(T)$ by two times at 80 K (curve *1* in Fig. 2, *a*). A similar behavior of rhombic distortion $\varepsilon_o(T)$ was observed earlier for a close compound, i.e., stoichiometric Er-cobaltite [34,35].

In case of substitution by Zn ions the magnitude of the rhombic strain step at T_S has a little increase, while the monotone changedecreases at lower temperatures. Thus, for the sample with $y = 0.3$ the magnitude of rhombic strain is maximum and equal to $\varepsilon_o \approx -5 \cdot 10^{-3}$. The change in parameter $\Delta c/c$ depending on y substitution by Zn ions demonstrates similar laws. The magnitude of step $\Delta c/c$ at T_S has a little increase, while the monotone change at lower temperatures decreases (Fig. 2, *b*). The steps in parameters $\Delta b/b$ and $\Delta c/c$ at phase transition are responsible for the small step in volume $\Delta V/V$, which is not measured reliably enough on the background of experimental data dispersion. It is worth noting, that diamagnetic dilution by Zn ions in the series of $YBaCo_{4-y}Zn_yO_{7+x}$ cobaltites affects the bulk strain in a different way, than the deviation from stoichiometry by oxygen, which is the target of research in Er-cobaltite [35,36].

To study the volume anomaly at phase transition in the series of $YBaCo_{4-y}Zn_yO_{7+x}$ cobaltites, the linear heat

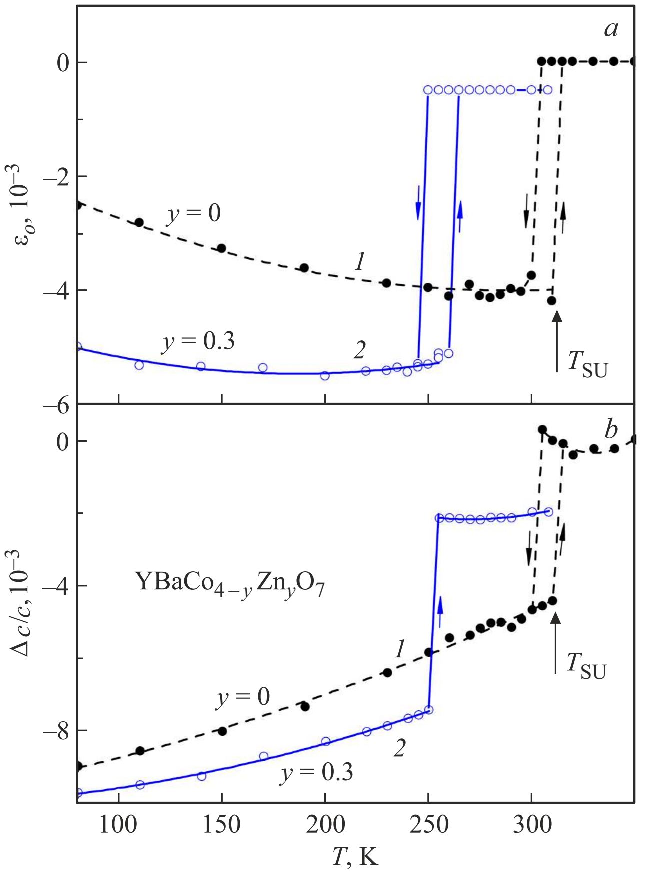

Figure 2. Changes a) in the degree of rhombic distortion $\varepsilon_o = (\Delta a/a - \Delta b/b)$ and b) of parameter $\Delta c/c(T)$ depending on temperature for stoichiometric substituted samples of $YBaCo_{4-y}Zn_yO_{7+x}$ with different dilution of Zn (curves *1* — $y = 0$, *2* — $y = 0.3$).

expansion was measured additionally by the strain-gauge method (Fig. 3). It can be seen that phase transition on pure $YBaCo_{4-y}O_{7+x}$ compound is accompanied by a positive step of $\Delta l/l_0 \approx 2 \cdot 10^{-4}$ while cooling. For the substituted sample the step has an opposite sign. It is characteristic, that heat expansion below the transition does not follow the Debye law, i.e., in addition to phonon, it has an additional magnetoelastic contribution (dashed line shows the extrapolation of the phonon contribution in the linear region). It is especially clearly seen in the case of sample with $y = 0.3$, where the derivative on curve $\Delta l/l_0(T)$ increases with temperature growth. At the same time the magnetoelastic contribution below T_S, as well as the step, has different sign for two samples, while above T_S their heat expansion is identical. To our opinion, this behavior is connected with the gradual development of a short-range magnetic order below T_S, and it was observed earlier for other thermodynamic properties as well, for example, heat capacity. With small lattice strains linear and volume expansion on a polycrystal without pronounced texture are related by the following relationship: $\Delta V/V_0 \approx 3\Delta l/l_0$, i.e., the volume anomaly at phase transition does not exceed 10^{-3}.

In the case of pure $YBaCo_{4-y}O_{7+x}$ compound below 100 K a negative heat expansion is observed due to magnetoelastic contribution caused by the establishment of long-range magnetic order (inset in Fig. 3). In the case of a sample with $y = 0.3$ this effect is weakly pronounced, because at a diamagnetic dilution of the Co-subsystem the temperature of magnetic ordering drops below 80 K.

In substituted and heterogeneous samples an issue arises regarding the determination of phase transition temperature from curves $\Delta l(T)/l_0$ (as well as from other thermodynamic properties). In pure homogenous samples a transition of the first kind is accompanied by a step on the curve $\Delta l(T)/l_0$, which, in case of positive step, is very close to the curve minimum. On the derivative curve $\alpha(T) = (1/l_0)l(T)/dT$ (heat expansion coefficient) these points correspond to the curve maximum and zero of its derivative. In case of nonstoichiometric or diluted samples, due to the heterogeneity of their composition over the volume, the anomalies are blurred and the above-mentioned characteristic temperatures on curves $\Delta l(T)/l_0$ and $\Delta(T)$ may be considerably different.

To determine the temperature of structural phase transition and hysteresis magnitude, we used temperature dependencies of linear expansion coefficient $\alpha(T)$ obtained by means of numerical differentiation with smoothing of experimental curves $\Delta l(T)/l_0$ (Fig. 4). In the case of a sample with $y = 0$, the temperature of transition $T_{SU} = 313$ K, which is well known from other properties, coincides

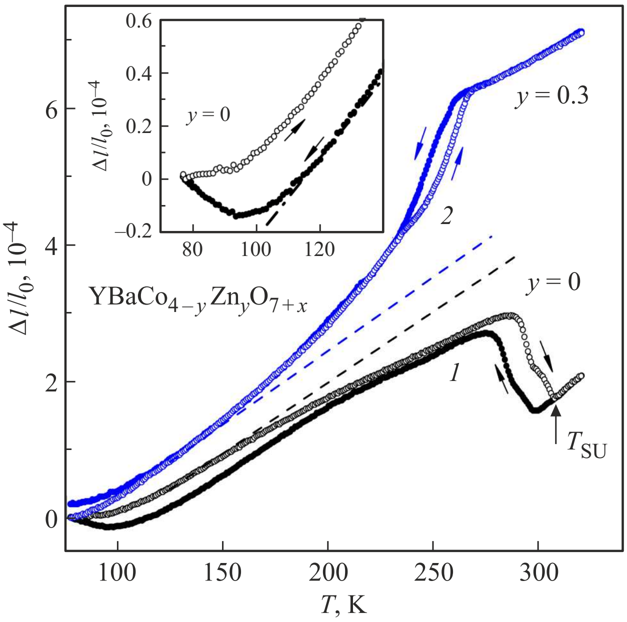

Figure 3. Linear heat expansion $\Delta l/l_0$ of stoichiometric substituted samples of $YBaCo_{4-y}Zn_yO_{7+x}$ with different dilution of Zn while heating (light dots) and cooling (dark dots) (curves *1* — $y = 0$, *2* — $y = 0.3$). The inset shows a region of magnetic transition for the sample with $y = 0$ in zoomed scale.

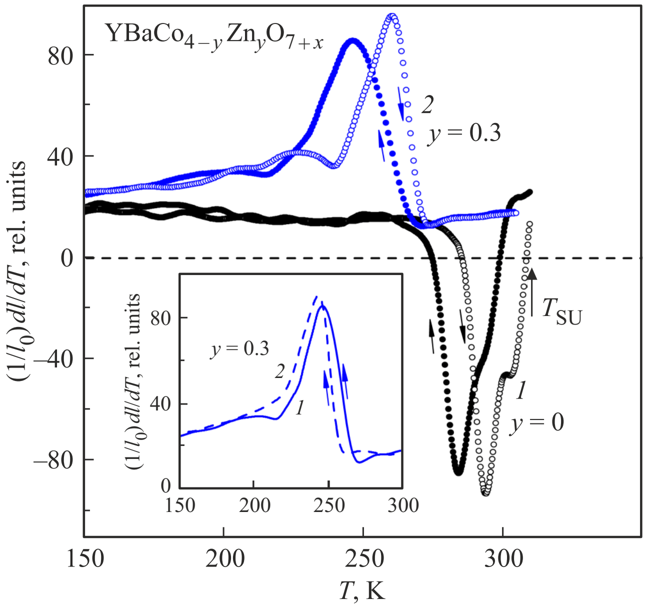

Figure 4. Temperature dependence of linear heat expansion coefficient $\alpha = (1/l_0)dl/dT$ of stoichiometric substituted samples of $YBaCo_{4-y}Zn_yO_{7+x}$ with different dilution of Zn while heating (light dots) and cooling (dark dots) (curves *1* — $y = 0$, *2* — $y = 0.3$) in the region of structural transition. The inset shows the impact of a magnetic field H on the linear expansion coefficient while cooling the sample with a Zn dilution of $y = 0.3$ (curves *1* — $H = 0$, *2* — $H = 2\,T$).

with the minimum/bend on the heat expansion dependence $\Delta l(T)/l_0$ (or zero of the heat expansion coefficient $\alpha(T)$). In the case of a sample with $y = 0.3$, that has a negative step at the transition this anomaly is closer to the top point of the bend on the curve $\Delta l(T)/l_0$ or to the middle of the step (maximum on curve $\alpha(T)$), corresponding to the most pronounced points on the curve $\Delta l(T)/l_0$. In the case of a sample with $y = 0.3$ the step is expanded over temperature (the maximum is wider), i.e., the transition is longer in time. The complex structure of extremes on curves $\alpha(T)$ may be indicative of either the heterogeneity of the sample, or the complex character of the structural transition itself. Unexpected is the noticeable (about 5 K) impact of magnetic field $H = 2\,T$ on the temperature of structural transition for the sample with $y = 0.3$ (inset in Fig. 4). Indeed, a noticeable impact of a magnetic field was observed earlier on the critical temperature for structural transitions of the Jahn-Teller nature with not very high T_S.

For the $YBaCo_{4-y}Zn_yO_{7+x}$ system, as well as for the series of $RBaCo_{4-y}O_{7+x}$ the experiment demonstrates a decrease in temperature T_S and an increase in anisotropic strain at the dilution of the cobalt subsystem or over the RE-series. While for the structural transitions of displacement type a relation is found between the transition temperature T_S and the angle of rotation φ_0 of tetrahedra at 0 K: $k_B T_S = K\varphi_0^2$ [26]. Thus, in case of decrease in temperature T_S a decrease in rotation angle φ_0 and rhombic strain connected with it should be expected.

3.2. Elastic properties of $YBaCo_{4-y}Zn_yO_{7+x}$ system

Additional information on the effect of dilution in the Co-subsystem by zinc ions on structural transitions can be received from measurements of elastic properties of the $YBaCo_{4-y}Zn_yO_{7+x}$ ($y = 0.1$, 0.3) series of compounds. Since the method of a composite vibrator is not suitable for the measurement at temperatures over 300 K, in the following we present the data for the samples with dilution of $y = 0.1$ and 0.3. For the ease of comparison the figures show relative changes in the absolute value of $\Delta E(T)/E_0$ ($\Delta E(T) = E(T) - E_0$; $E_0 = E(T = 300\,K)$) normalized to the value of E_0 at $T = 300\,K$ (Fig. 5). Curves $\Delta E(T)/E_0$ are obtained after several cycles of thermocycling at slow cooling (dark dots) and slow heating (light dots).

The presence of softening, pronounced minimum, and considerable hysteresis on the curve $\Delta E(T)/E_0$ with a

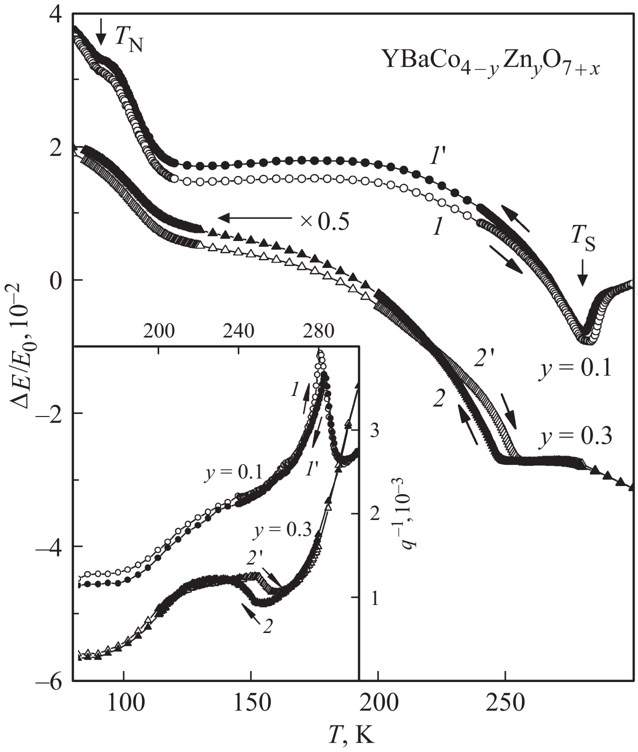

Figure 5. Dependencies of the relative Young modulus $\Delta E/E_0$ on temperature for stoichiometric substituted samples of $YBaCo_{4-y}Zn_yO_{7+x}$ with different Zn dilution (curve *1* and *1'* — $y = 0.1$, *2* and *2'* — $y = 0.3$; scale along the vertical axis for curves *2, 2'* is zoomed out by 2 times) while heating (light dots) and cooling (dark dots; curves for different samples are arbitrarily shifted along the vertical axis). The inset shows temperature dependence of internal friction coefficient $q^{-1}(T)$ for these samples (curves *1* and *1'* — $y = 0.1$, *2* and *2'* — $y = 0.3$) while heating (light dots) and cooling (dark dots) in the region of structural transition.

decrease in temperature are indicative of the phase transition. With an increase in dilution of the cobalt subsystems a decrease in minima and their shift towards lower temperatures are observed on curves $\Delta E(T)/E_0$ (Fig. 5). Temperatures of local minima attributable to structural transitions for samples with $y = 0.1$ and 0.3 while heating T_{SU} and cooling T_{SD} are below 300 K, i.e., there is no distortion of structure at a room temperature. It is worth noting, that no pronounced minima and anomalies in a temperature range of 200−280 K were observed for any quenched nonstoichiometric samples. Pronounced minima and hysteresis loops are seen for all samples after annealing.

A change in transition temperature for the samples with dilution of the cobalt subsystem by Zn^{2+} ions can be also observed on temperature dependencies of internal friction coefficient $q^{-1}(T)$ (insert in Fig. 5). For the sample with $y = 0.1$ a λ-anomaly on the curve $q^{-1}(T)$ is observed in a temperature range of 275−285 K, while for the sample with $y = 0.3$ this anomaly is blurred and becomes a step.

Thus, it follows from the elastic properties that there is a structural transition in annealed stoichiometric samples of $\mathrm{YBaCo}_{4-y}\mathrm{Zn}_y\mathrm{O}_{7+x}$, which match the X-ray data and results of heat expansion measurements. It is worth noting, that T_{SU} and T_{SD} determined from X-ray data and from measurements of elastic properties and heat expansion are slightly different. X-ray data define stability boundaries of symmetrical and asymmetrical phases, while corresponding anomalies on curves $\Delta E(T)/E_0$ and $\Delta l(T)/l_0$ define temperatures at which low-temperature and high-temperature phases have the largest volume.

4. Conclusion

In this work we studied the change in characteristics of structural phase transition in case of substitution of Co ions with Zn ions in a series of cobaltites $\mathrm{YBaCo}_{4-y}\mathrm{Zn}_y\mathrm{O}_{7+x}$ ($y = 0$, 0.3). According to X-ray studies, for a pure sample of $\mathrm{YBaCo}_{4-y}\mathrm{O}_{7+x}$ at the structural transition parameter $\Delta a/a$ does not demonstrate any features, parameters b and c undergo steps with different signs and different magnitudes, which results in a change in the c/a_{av} ratio for the structure and a volume step of $\Delta V/V \sim -1 \cdot 10^{-3}$. Also, similar anomalies are observed for structure parameters of the substituted sample of $\mathrm{YBaCo}_{4-y}\mathrm{Zn}_y\mathrm{O}_{7+x}$ with $y = 0.3$. Measurements of heat expansion has confirmed, that the transition is accompanied by a step in the volume of the lattice cell $\Delta V/V \approx 10^{-3}$, which has a different sign for samples with $y = 0$ and $y = 0.3$.

The change in the step sign may be connected with different deviations from stoichiometry over oxygen in the samples under study. This effect was observed earlier for $\mathrm{ErBaCo}_{4-y}\mathrm{O}_{7+x}$ cobaltites [34,35]. According to our X-ray data, at a slight deviation from stoichiometry ($x < 0.05$ for quenched samples) the rhombic distortion changes insignificantly, while the biggest change is undergone by the volume anomaly that changes its sign. The temperature of the structural transition T_{SU} and T_{SD} drops in a monotone manner and almost linearly with an increase in substitution y, i.e., with an increase in lattice parameters a and c. It is well known that in case of substitution in the $R\mathrm{BaCo}_{4-y}\mathrm{O}_{7+x}$ rare-earth subsystem the temperature of structural transition, on the contrary, grows with an increase in lattice parameters a and c .

Distortion of the structure is accompanied by pronounced anomalies of the Young modulus $\Delta E(T)/E_0$ and internal friction $q^{-1}(T)$ in substituted annealed samples. The substitution by ions of Zn results in a qualitative change in the character of the Young modulus anomaly in the region of T_{S}, namely in a sharp decrease in the step on the curve $\Delta E(T)/E_0$ followed by the full removal of this step. It may be connected with a change in the ratio between isotropic and anisotropic strain at the structural transition with a small substitution in the cobalt subsystem, because contributions of these strains in the Young moduli are different [35,36]. The dilution of the cobalt subsystem and deviation from stoichiometry have different effects on the structure distortion and elastic properties.

Currently there is no commonly held opinion regarding the mechanism of structural transition in RE-cobaltites and various models are discussed, such as charge ordering in the Co-subsystem, optimization of unsaturated bonds of Ba-coordination polyhedron or violation of the tolerance condition for the structure. The obtained information about structure distortion at phase transition is indicative of a decrease in the lattice parameters ratio c/a_{av}, that can be an important factor for the stability of the structure.

Distortion of the structure at phase transition in the $\mathrm{YBaCo}_{4-y}\mathrm{Zn}_y\mathrm{O}_{7+x}$ series of cobaltites removes the frustration of exchange interactions and should promote the subsequent establishment of a long-range magnetic order in a cobalt subsystem at $T_{\mathrm{N}} < T_{\mathrm{S}}$ [17,18]. This issue should be a target of further separate research.

Conflict of interest

The authors declare that they have no conflict of interest.

References

[1] P. Schiffer, A.P. Ramirez. Commun. Condens. Mater. Phys. **18**, *1*, 21 (1996).

[2] M.J. Harris, M.P. Zinkin. Mod. Phys. Lett. B **10**, *10*, 417 (1996).

[3] J.N. Reimers, A.J. Berlinsky. Phys. Rev. B **48**, *13*, 9539 (1993).

[4] P. Lecheminant, B. Bernu, C. Lhuillier, L. Pierre, P. Sindzingre. Phys. Rev. B **56**, *5*, 2521 (1997).

[5] L.C. Chapon, P.G. Radaelli, H. Zheng, J.F. Mitchell. Phys. Rev. B **74**, *17*, 172401 (2006).

[6] P. Manuel, L.C. Chapon, P.G. Radaelli, H. Zheng, J.F. Mitchell. Phys. Rev. Lett. **103**, *3*, 037202 (2009).

[7] W. Schweika, M. Valldor, P. Lemmens. Phys. Rev. Lett. **98**, *6*, 067201 (2007).

[8] V. Caignaert, V. Pralong, A. Maignan, B. Raveau. Solid State Commun. **149**, *11–12*, 453 (2009).

[9] V. Caignaert, V. Pralong, V. Hardy, C. Ritter, B. Raveau. Phys. Rev. B **81**, *9*, 094417 (2010).

[10] K. Singh, V. Caignaert, L.C. Chapon, V. Pralong, B. Raveau, A. Maignan. Phys. Rev. B **86**, *2*, 024410 (2012).

[11] E.A. Juarez-Arellano, A. Friedrich, D.J. Wilson, L. Wiehl, W. Morgenroth, B. Winkler, M. Avdeev, R.B. Macquart, C.D. Ling. Phys. Rev. B **79**, *6*, 064109 (2009).

[12] E.V. Tsipis, J.C. Waerenborgh, M. Avdeev, V.V. Kharton. J. Solid State Chem. **182**, *3*, 640 (2009).

[13] L.P. Kozeeva, N.V. Kameneva, M.Yu. Smolentsev, A.I. Danilovich, V.S. Podberezskaya. Zhurn. strukt. khimii **49**, *6*, 1109 (2008) (in Russian).

[14] A. Huq, J.F. Mitchell, H. Zheng, L.C. Chapon, P.G. Radaelli, K.S. Knight, P.W. Stephens. J. Solid State Chem. **179**, *4*, 1136 (2006).

[15] D.D. Khalyavin, L.C. Chapon, P.G. Radaelli, H. Zheng, J.F. Mitchell. Phys. Rev. B **80**, *14*, 144107 (2009).

[16] D.D. Khalyavin, P. Manuel, B. Ouladdiaf, A. Huq, P.W. Stephens, H. Zheng, L.C. Chapon. Phys. Rev. B **83**, *9*, 094412 (2011).

[17] M. Markina, A.N. Vasiliev, N. Nakayama, T. Mizota, Y. Yeda. J. Magn. Magn. Mater. **322**, *9–12*, 1249 (2010).

[18] M. Valldor, Y. Sanders, W. Schweika. J. Phys.: Conf. Ser. **145**, *1*, 012076 (2009).

[19] N. Nakayama, T. Mizota, Y. Ueda, A.N. Sokolov, A.N. Vasiliev. J. Magn. Magn. Mater. **300**, *1*, 98 (2006).

[20] V. Caignaert, A. Maignan, K. Singh, C. Simon, V. Pralong, B. Raveau, J.F. Mitchell, H. Zheng, A. Huq, L.C. Chapon. Phys. Rev. B **88**, *17*, 174403 (2013).

[21] A. Maignan, V. Caignaert, D. Pelloquin, S. Hébert, V. Pralong, J. Hejtmanek, D. Khomskii. Phys. Rev. B **74**, *16*, 165110 (2006).

[22] Z.A. Kazey, V.V. Snegiryov, A.S. Andreenko, L.P. Kozeeva. ZhETF **140**, *2*, 282 (2011) (in Russian).

[23] Z. Kazei, V. Snegirev, A. Andreenko, L. Kozeeva, M. Kameneva. Solid State Phenomena **233**, 145 (2015).

[24] M. Soda, Y. Yasui, T. Moyoshi, M. Sato, N. Igawa, K. Kakurai. J. Phys. Soc. Jpn. **75**, *5*, 054707 (2006).

[25] A.I. Rykov, Y. Ueda, M. Isobe, N. Nakayama, Y.T. Pavlyukhin, S.A. Petrov, A.N. Shmakov, V.N. Kriventsov, A.N. Vasiliev. New J. Phys. **12**, *4*, 043035 (2010).

[26] M.T. Dove, M. Gambhir, K.D. Hammonds, V. Heine, A.K. Pryde. Phase Transitions **58**, *1–3*, 121 (1996).

[27] A.I. Rykov, K. Nomura, T. Mitsui, M. Seto. Physica B: Condens. Matter **350**, *4*, 287 (2004).

[28] H. Boysen, B. Dorner, F. Frey, H. Grimm. J. Phys. C **13**, *33*, 6127 (1980).

[29] Z.A. Kazey, V.V. Snegiryov, L.P. Kozeeva, M.Yu. Kameneva, A.N. Lavrov. ZhETF **153**, *5*, 782 (2018) (in Russian).

[30] L.P. Kozeeva, M.Yu. Kameneva, A.N. Lavrov, N.V. Podberezskaya. Neorgan. materialy **49**, *6*, 668 (2013) (in Russian).

[31] A.V. Alekseev, M.Yu. Kameneva, L.P. Kozeeva. Izv. RAN. Ser. fiz. **77**, *2*, 173 (2013) (in Russian).

[32] M. Karppinen, M. Matvejeff, K. Salomäki, H. Yamauchi. J. Mater. Chem. **12**, *6*, 1761 (2002).

[33] Z.A. Kazey, V.V. Snegiryov, M.S. Stolyarenko. Pis'ma v ZhETF **112**, *3*, 189 (2020) (in Russian).

[34] Z.A. Kazey, V.V. Snegiryov, M.S. Stolyarenko. ZhETF **160**, *5*, 689 (2021) (in Russian).

[35] M. Fukuhara, M. Yagi, A. Matsuo. Phys. Rev. B **65**, *22*, 224210 (2002).

[36] L.R. Testardi. Phys. Rev. B **12**, *9*, 3849 (1975).